Experimental Neurology 347 (2022) 113896

Contents lists available at ScienceDirect

Experimental Neurology

journal homepage: www.elsevier.com/locate/yexnr

Research paper

Selective expression of the neurexin substrate for presenilin in the adult forebrain causes deficits in associative memory and presynaptic plasticity

Ana C. Sánchez-Hidalgo [a,b,1], Francisco Arias-Aragón [a,b], M. Teresa Romero-Barragán [c], Celia Martín-Cuevas [a,b,1], José M. Delgado-García [c], Amalia Martinez-Mir [a], Francisco G. Scholl [a,b,*]

[a] Instituto de Biomedicina de Sevilla (IBiS), Hospital Universitario Virgen del Rocío/CSIC/Universidad de Sevilla, Avda. Manuel Siurot s/n, Sevilla 41013, Spain
[b] Departamento de Fisiología Médica y Biofísica, Facultad de Medicina, Universidad de Sevilla, Avda. Sánchez Pizjuán, 4, Sevilla 41009, Spain
[c] Division of Neurosciences, Pablo de Olavide University, Seville 41013, Spain

ARTICLE INFO

Keywords:
Neurexin
Presenilin
Alzheimer's disease
Synapse
Synaptic plasticity
Memory

ABSTRACT

Presenilins (PS) form the active subunit of the gamma-secretase complex, which mediates the proteolytic clearance of a broad variety of type-I plasma membrane proteins. Loss-of-function mutations in *PSEN1/2* genes are the leading cause of familial Alzheimer's disease (fAD). However, the PS/gamma-secretase substrates relevant for the neuronal deficits associated with a loss of PS function are not completely known. The members of the neurexin (Nrxn) family of presynaptic plasma membrane proteins are candidates to mediate aspects of the synaptic and memory deficits associated with a loss of PS function. Previous work has shown that fAD-linked PS mutants or inactivation of PS by genetic and pharmacological approaches failed to clear Nrxn C-terminal fragments (NrxnCTF), leading to its abnormal accumulation at presynaptic terminals. Here, we generated transgenic mice that selectively recreate the presynaptic accumulation of NrxnCTF in adult forebrain neurons, leaving unaltered the function of PS/gamma-secretase complex towards other substrates. Behavioral characterization identified selective impairments in NrxnCTF mice, including decreased fear-conditioning memory. Electrophysiological recordings in medial prefrontal cortex-basolateral amygdala (mPFC-BLA) of behaving mice showed normal synaptic transmission and uncovered specific defects in synaptic facilitation. These data functionally link the accumulation of NrxnCTF with defects in associative memory and short-term synaptic plasticity, pointing at impaired clearance of NrxnCTF as a new mediator in AD.

1. Introduction

Neurexins (Nrxns) form a large family of presynaptic adhesion proteins that couple neurotransmitter release and trans-synaptic interactions with postsynaptic ligands (Dean et al., 2003; Südhof, 2017). Genetic studies and analysis of protein levels in peripheral samples from patients suggest a role for altered Nrxn levels in preclinical and clinical stages of Alzheimer's disease (AD) (Duits et al., 2018; Goetzl et al., 2018; Lleó et al., 2019; Martinez-Mir et al., 2013). Nrxns are subject to regulation at several levels. At the transcriptional level, the use of alternative promoters together with extensive alternative splicing generates hundreds of isoforms that differ at the extracellular domain (Gomez et al., 2021; Schreiner et al., 2014; Treutlein et al., 2014). Proteolytic cleavage is emerging as a new post-translational mechanism that regulates Nrxn function (Saura et al., 2011; Servián-Morilla et al., 2018). Proteolytic regulation of Nrxns proceeds in two sequential steps. First, a cleavage in the juxtamembrane region releases the specific ectodomain of the processed isoform and generates a common membrane-bound Nrxn C-terminal fragment (NrxnCTF) (Saura et al., 2011). Subsequently, NrxnCTF is cleared by Presenilins (PS), the active subunit of the gamma-secretase complex, which mediates the intramembrane cleavage of a number of substrates (Bot et al., 2011; Saura et al., 2011; Servián-Morilla et al., 2018). Importantly, mutations in *PSEN1/2* genes are the main cause of familial AD (fAD) explaining about 90% of fAD cases (Cacace et al., 2016).

Several findings support that fAD-linked *PSEN* mutations act trough

* Corresponding author at: Instituto de Biomedicina de Sevilla (IBiS), Campus del Hospital Universitario Virgen del Rocío, Avda. Manuel Siurot s/n, Sevilla 41013, Spain.
E-mail address: fgs@us.es (F.G. Scholl).
[1] Present address: Spanish Network for Research in Mental Health (CIBERSAM), Monforte de Lemos AV, 3–5, Madrid 28029, Spain.

https://doi.org/10.1016/j.expneurol.2021.113896
Received 2 July 2021; Received in revised form 27 September 2021; Accepted 10 October 2021
Available online 15 October 2021

a loss-of-function mechanism (De Strooper, 2007; Shen and Kelleher 3rd, 2007; Wolfe, 2007). In a seminal study, Shen and collaborators showed that conditional mice lacking PS1/2 genes in adult forebrain neurons (PScKO mice) develop key symptoms resembling AD, including early and progressive deficits in synaptic plasticity and memory, followed by late synapse loss, neurodegeneration and hyperphosphorylation of Tau proteins (Saura et al., 2004). Biochemical evaluation of fAD-associated gamma-secretase complexes and the generation of mouse models recapitulating fAD-linked *PSEN1* mutations have further supported the loss-of-function hypothesis for PS in AD (Sun et al., 2017; Xia et al., 2015; Zhou et al., 2017). As such, loss of PS function results in decreased gamma-secretase activity inducing the accumulation of its proteolytic substrates in a context-dependent manner. Thus, the accumulation of a particular substrate coinciding with the onset of symptoms helps to define potential candidates associated with impaired PS function. However, the high number of substrates for PS/gamma-secretase challenges the identification of single candidates with a functional relevance in the loss of PS function (Güner and Lichtenthaler, 2020; Haapasalo and Kovacs, 2011). Therefore, the PS/gamma-secretase substrates that can produce key synaptic and memory defects associated with a loss of PS function are not completely known.

Nrxns are candidates to mediate aspects of the synaptic and behavioral deficits caused by loss of PS/gamma-secretase function. It has been previously shown that chemical or genetic inhibition of PS/gamma-secretase activity results in the accumulation of NrxnCTF *in vitro* and *in vivo* (Bot et al., 2011; Saura et al., 2011). Moreover, the clearance of NrxnCTF is inhibited in cells expressing fAD-associated *PSEN1* mutations, suggesting that NrxnCTF accumulates in fAD (Bot et al., 2011; Saura et al., 2011). *In vivo*, NrxnCTF accumulates at presynaptic terminals of PScKO mice at a time coinciding with the onset of synaptic and behavioral deficits but prior to neurodegeneration (Saura et al., 2011). Importantly, the sole expression of NrxnCTF in cultured hippocampal neurons while maintaining PS function mimics the deficits in neurotransmitter release and calcium influx caused by the absence of PS1/2 genes or gamma-secretase activity (Servián-Morilla et al., 2018). Although these findings suggested a role for the impaired synaptic clearance of NrxnCTF in the loss of PS function, the deficits produced by the brain accumulation of NrxnCTF are currently unknown.

In this study, we generated transgenic mice that selectively accumulate NrxnCTF in adult forebrain neurons. Biochemical characterization showed that NrxnCTF mice recapitulate the distribution of NrxnCTF found in conditional mice lacking PS1/2 function in the forebrain. However, PS/gamma-secretase function towards other substrates is not affected in NrxnCTF mice. Importantly, we found that the selective accumulation of NrxnCTF produces behavioral deficits, including decreased fear-conditioning memory. Electrophysiological recordings in alert behaving mice revealed impaired short-term synaptic plasticity at mPFC-BLA synapses of NrxnCTF mice, in line with the presence of a putative presynaptic mechanism. These data indicate that the impaired synaptic clearance of NrxnCTF caused by a loss of PS function leads to synaptic plasticity and behavioral deficits in mature brain.

2. Materials and methods

2.1. Generation of transgenic NrxnCTF mice

The HA-NrxnCTF construct contains a signal peptide followed by a HA tag and the last 85C-terminal residues of human Nrxn1. A DNA fragment containing the TRE promoter, the coding sequence of HA-NrxnCTF and a WPRE fragment (woodchuck hepatitis virus post-transcriptional regulatory element) was injected into the pronucleus of FVB/N zygote for transgenic mouse production. TRE-NrxnCTF mouse lines were mated with CaMKIIα-tTA mice (Mayford et al., 1996) in a C57BL/6 *J* background. Doxycycline (DOX) was provided in the diet (SAFE, 40 mg/kg). PScKO^{tam} mice were generated by crossing fPS1/fPS1;PS2−/− with CaMKIIα-CreERT2 mice (Erdmann et al., 2007). Generation and characterization of fPS1/fPS1;PS2−/− mice have been previously described (Saura et al., 2004; Shen et al., 1997). Animals were kept at 22 °C on a 12 h dark/light cycle and food and water were provided *ad libitum*. Mice were used according to animal care standards and all protocols were approved by the Committee of Animal Use for Research at the University of Seville (Spain).

2.2. Biochemical analysis

Forebrain tissues were homogenized in lysis buffer (50 mM Tris-HCl pH 7.4; 100 mM NaCl; 5 mM MgCl2; 1% Triton X-100 and 0.1% SDS) containing a protease inhibitor cocktail (Roche). Synaptosome fractions were isolated as previously described (Carlin et al., 1980; Saura et al., 2011). In brief, tissues from 5-6-month-old mice (three animals per preparation) were homogenized with a Teflon-glass homogenizer in buffer A (5 mM HEPES pH 7.4, 0.32 M sucrose, 1 mM NaHCO3, 1 mM MgCl2, 0.5 mM CaCl2, 0.1% NP-40) supplemented with protease and phosphatase inhibitors cocktail (Sigma). The resulting homogenate (L fraction) was centrifuged at 1400*g* for 10 min. The supernatant was saved (S1) and the pellet was further homogenized in buffer A and centrifuged at 710*g* for 10 min. The supernatants (S1 and S2) were combined and centrifuged (13,800 *g* for 10 min). The pellet was resuspended in buffer B (6 mM Tris HCl pH 8.0, 0.32 M sucrose, 1 mM NaHCO3, 0.1% NP40, with phosphatase and protease inhibitors), homogenized (M fraction) and loaded on top of an ice-cold discontinuous sucrose gradient (1.2 M, 1 M and 0.85 M) and centrifuged at 82,500 *g* for 2 h. Synaptosome fraction (S fraction) was collected from the interface between 1 M and 1.2 M layers, diluted in buffer C (12 mM Tris pH 8.0, 1% Triton X-100, with phosphatase and protease inhibitors) and incubated on ice for 15 min. The suspension was centrifuged at 32,800 *g* for 1 h. The supernatant was collected (presynaptic fraction) and the pellet was resuspended and sonicated in buffer D (40 mM Tris pH 8.0, 1% NP-40, with phosphatase and protease inhibitors) to obtain the postsynaptic fraction. All steps were performed at 4 °C. Fractions were aliquoted, frozen in liquid N_2 and stored at −80 °C. Protein concentration was determined with the BCA protein assay kit (Pierce).

Western blot experiments of lysates containing equal-protein loading (15-40 μg per lysate) were performed using the following primary antibodies: rat anti-HA (1:500, Roche), rabbit anti-Neurexin 1,2,3 (1:500, Synaptic Systems), mouse anti-PSD95 (1:1000, ThermoScientific), mouse anti-SNAP25 (1:2000, Sigma Aldrich) and mouse anti-β actin (1:5000, Sigma Aldrich). Immunoreactivity was detected with appropriate secondary antibodies conjugated with horseradish peroxidase (1:5000, Jackson ImmunoResearch). Chemiluminescence was developed using Clarity ECL Substrate (Bio-Rad) or Clarity Max ECL Substrate (Bio-Rad) on an ImageQuant LAS4000 Mini (GE Healthcare Life Sciences).

2.3. Behavioral analysis

Behavioral studies were performed in two independent cohorts of male NrxnCTF and littermate control (wild-type, TRE-NrxnCTF and CaMKIIα-tTA) mice of the same age (5–8 months). To elude early transgene expression, all mice were fed with diet with DOX from gestation to 30 days after birth. Mice were caged in the behavioral room for 30 min before the behavioral examination. Tests were carried out from 9 a.m. to 6 p.m. All behavioral tasks and quantification analysis were performed by researchers blind to the genotype of the mice.

2.4. Open field test

The tested mouse was allowed to freely explore a square open field arena (45 × 45 cm, Harvard Apparatus) for 15 min. Automatic detection of the mouse, total travelled distance and time spent in the central zone (20 cm apart from the walls) were recorded with the Smart software

(PanLab).

2.5. Self-grooming

Stereotyped behavior was studied with the self-grooming test. Mice were placed in a clean cage without bedding. After 10 min of habituation, behavior was video-recorded for 10 min. Time spent in self-grooming and numbers of bouts were manually quantified.

2.6. Three-chamber test

The test was performed as described previously (Silverman et al., 2010) with minor modifications. A social interaction box (Harvard Apparatus) divided in 3 compartments was used. The social arena was made of a transparent box (42 × 60 cm) with two transparent sliding doors that divide left, right and center chambers (42 × 20 cm). In the first 10-min session, the tested mouse was placed in the central chamber with the sliding doors closed. Then, a 10-min habituation session proceeded where the tested mouse had access to the sided chambers, containing two empty circular cages (8 cm diameter). After habituation, circular cages housing an unfamiliar C57BL/6 J mouse of the same sex and age or an inanimate object (plastic cube) was located in the corners of the left or right chambers. A cylindrical bottle filled with water was placed on top of the enclosures to prevent the tested mouse from climbing. The tested mouse was located in the central chamber and allowed to explore the arena for 10 min. The location of the cages was alternated between tests. Tests were video-recorded and the number of transitions between compartments was automatically registered with the Smart software. Time spent in close contact with the cages was manually measured.

2.7. Novel object recognition and Barnes maze tests

The tested mouse was placed in the center of the open field arena and allowed to freely explore the area for 15 min. Following habituation to the arena, two identical objects were placed in opposite corners, 15 cm apart from the walls. The tested mouse was placed back in the center of the field and allowed to explore the area for 10 min. After 24 h, one of the familiar objects was replaced for a new object of different size, colour and shape. Then, the tested mouse was placed in the arena and allowed to explore the area for 10 min. The location of the new object was alternated between assays. The test was video-recorded and the time spent interacting with the objects was manually measured.

The Barnes maze assay was performed as previously described (Andrade-Talavera et al., 2015). Briefly, mice were located on top of an elevated round platform (Harvard Apparatus) delimited by 20 evenly spaced holes in the periphery. To assess spatial memory, visuo-spatial cues were located hanging on panels in the proximity surrounding the platform. During learning, all holes but one, the escape hole, were covered and mice were exposed to the platform. Bright light and standing fans serve as motivating factors to induce scape behavior. The escape hole is maintained at a fixed location for the duration of training, which involves four daily trials (maximum time to find the escape hole: 180 s per trial). In unsuccessful trials, mice were gently guided to the escape hole at the end of the trial. Twenty-four hours and eight days after training, mice were tested in a single session of 90 s in the same set-up with all holes covered. The time in reaching the escape hole and spent in each quadrant was automatically quantified (SMART software).

2.8. Fear conditioning test

The contextual and auditory fear-conditioning test was evaluated in a test box (Harvard Apparatus). Mice were allowed to freely explore the test box for 2 min before they were exposed to conditioning phase consisting of three repetitions of a 30 s tone co-terminating for 2 s with a mild electric shock (0.2 mA). After 24 h, mice were placed in the same conditioning room for 5 min (contextual phase). Then, mice were exposed to three repetitions of the tone but in a different shaped chamber and without a shock. Freezing response during the tests was detected with sensors located in the floor. *Packwin* software was used to automatically analyze the freezing response.

2.9. Surgery

For electrode implantation, mice were anaesthetized with 1–2% isoflurane, supplied from a calibrated Fluotec 5 (Fluotec-Ohmeda, Tewksbury, MA, USA) vaporizer, at a flow rate of 1–2 L/min oxygen (AstraZeneca, Madrid, Spain) and placed into a stereotaxic frame. Additional anesthesia was delivered by a special mouse mask (David Kopf Instruments, Tujunga, CA). Animals were implanted with a bipolar stimulating electrode in the medial prefrontal cortex (mPFC) (1.8 mm rostral to Bregma; 0.3 mm lateral; and 2 mm deep from the brain's surface) (Franklin and Paxinos, 2007) and a bipolar recording electrode in the basolateral amygdala (BLA) (1.8 mm posterior to Bregma; 3 mm lateral; and 3.9 mm deep from the brain's surface). Electrodes were made of 50 μm, Teflon-coated, tungsten wires (Advent Research, Eynsham, UK) and their tip were bared of their isolating cover for 0.5 mm. Two screws, each one connected to a bare silver wire, were affixed to the skull as a ground. The six wires were soldered to a 6-pin socket (RS Amidata, Madrid, Spain), which was covered and fixed to the brain with dental cement. Further information about this experimental procedure is detailed elsewhere (Gruart et al., 2006). After surgery, animals recovered for a week before the start of the recording sessions.

2.10. Stimulation and recording procedures

Recording sessions were carried out in 6 mice at a time. Animals were placed in individual small (5 cm × 5 cm × 10 cm) plastic chambers located inside a larger Faraday box (30 cm × 30 cm × 20 cm). Field excitatory postsynaptic potentials (fEPSPs) were evoked with the help of Cibertec CS20 stimulators (Cibertec, Madrid, Spain) and recorded with Dagan Corporation EX4-400 Quad Differential amplifiers (Dagan Corporation, Minneapolis MN USA) at a bandwidth of 0.1 Hz-10 kHz, through a high-impedance probe (2×10^{12} Ω, 10 pF).

2.11. Paired-pulse facilitation and input/output curves

Input/output curves were tested with paired pulses (40 ms of inter-stimulus interval) of increasing intensities (0.02–0.4 mA, in steps of 0.02 mA). Animals received ten pulses for each intensity, which were averaged in order to measure the evoked fEPSP amplitude. For the paired-pulse facilitation test, 17 mice were stimulated with paired pulses of different inter-stimulus intervals (10, 20, 40, 100, 200 and 500 ms; ten pulses each) with intensities corresponding to 40% of the intensity necessary to evoke a saturating fEPSP response.

2.12. Long-term potentiation

Baseline recordings were carried out for 15 min prior to the LTP induction. Field EPSPs were evoked with paired (40 ms inter-stimulus interval) 100 μs squared, biphasic pulses at a rate of 3/min (0.05 Hz). Pulse intensity was set at 40% of the amount necessary to evoke a maximum fEPSP response (0.05–8.0 mA) (Gruart et al., 2006; Gureviciene et al., 2004). LTP was induced by applying a high-frequency stimulation (HFS) protocol, which consisted of five 100 ms trains of pulses at a frequency of 200 Hz presented at a rate of one per second. This protocol was presented 6 times (1/min). In order to avoid evoking large population spikes and/or the appearance of EEG seizures, the stimulus intensity during the HFS was set at the same value as that used for generating baseline recordings. None of the animals used in this study presented any after-discharge or motor seizure following the HFS protocol, as checked by on-line EEG recordings and visual observation of

the stimulated mouse (Madroñal et al., 2009). After the induction, fEPSPs were recorded with the same procedure of the baseline along four sessions (1 h in day 1 and 30 min in days 2–4). Field EPSP amplitude was measured in the recordings before and after evoking long-term potentiation (LTP) and represented as a percentage of the base line (taken as a 100%), calculating the average of 15 pulses for each 5 min interval.

2.13. Histology

At the end of the recording sessions, mice were deeply anaesthetized (sodium pentobarbital, 50 mg/kg) and perfused transcardially with 0.9% saline followed by fixation with 4% paraformaldehyde in phosphate-buffer (PFA). Brains were removed from the skull and maintained in PFA overnight at 4 °C and cryoprotected with an increasing gradient (5–30%) of sucrose in PBS. 50 μm brain slices was obtained with a cryotome (Leica, Wetzlar, Germany). Brain sections with the structures of interest were mounted on gelatinized glass slides and stained using a Nissl technique (0.1% Toluidine Blue). Micrographs of the electrode scar were taken with a light microscope.

2.14. Data collection and analysis

Behavioral tests were video-recorded and manually or automatically quantified and data were analyzed using one-way ANOVA with Tukey post-hoc test. Field EPSPs were stored digitally on a computer through the analogue/digital converter CED 1401 Plus (CED, Cambridge, England), at a sampling frequency of 5 kHz with an amplitude resolution of 16 bits. Data were analyzed off-line for fEPSP amplitude with the help of CED Spike 2 and Signal (Systat Software, San Jose, CA, USA) programs. For this, 15 successive fEPSPs were averaged every 5 min to quantify EPSP amplitudes. Results were represented with Microsoft Excel (Microsoft, Redmon, WA, USA) and CorelDraw (Corel Corporation, Ottawa, Canada) programs and computed and processed for statistical analysis using the Sigma Stat for Windows package. Regression analyses were used to study the relationship between LTP and paired-pulse variables (Student's *t*-test). Unless otherwise indicated, data are represented as the mean ± SEM. Acquired data were analyzed using a two-way ANOVA, with sessions as repeated measure. Contrast analysis was added for a further study of significant differences.

3. Results

3.1. Generation of mice expressing NrxnCTF in the forebrain

The accumulation of NrxnCTF in mice lacking PS1/2 genes in the adult forebrain suggests a contribution of the impaired processing of Nrxns in the neuronal defects caused by a loss of gamma-secretase function. However, the broad accumulation of substrates following inhibition of PS/gamma-secretase activity avoids the identification of single substrates with a functional impact. To face this limitation, we have developed transgenic mice that selectively accumulate NrxnCTF in

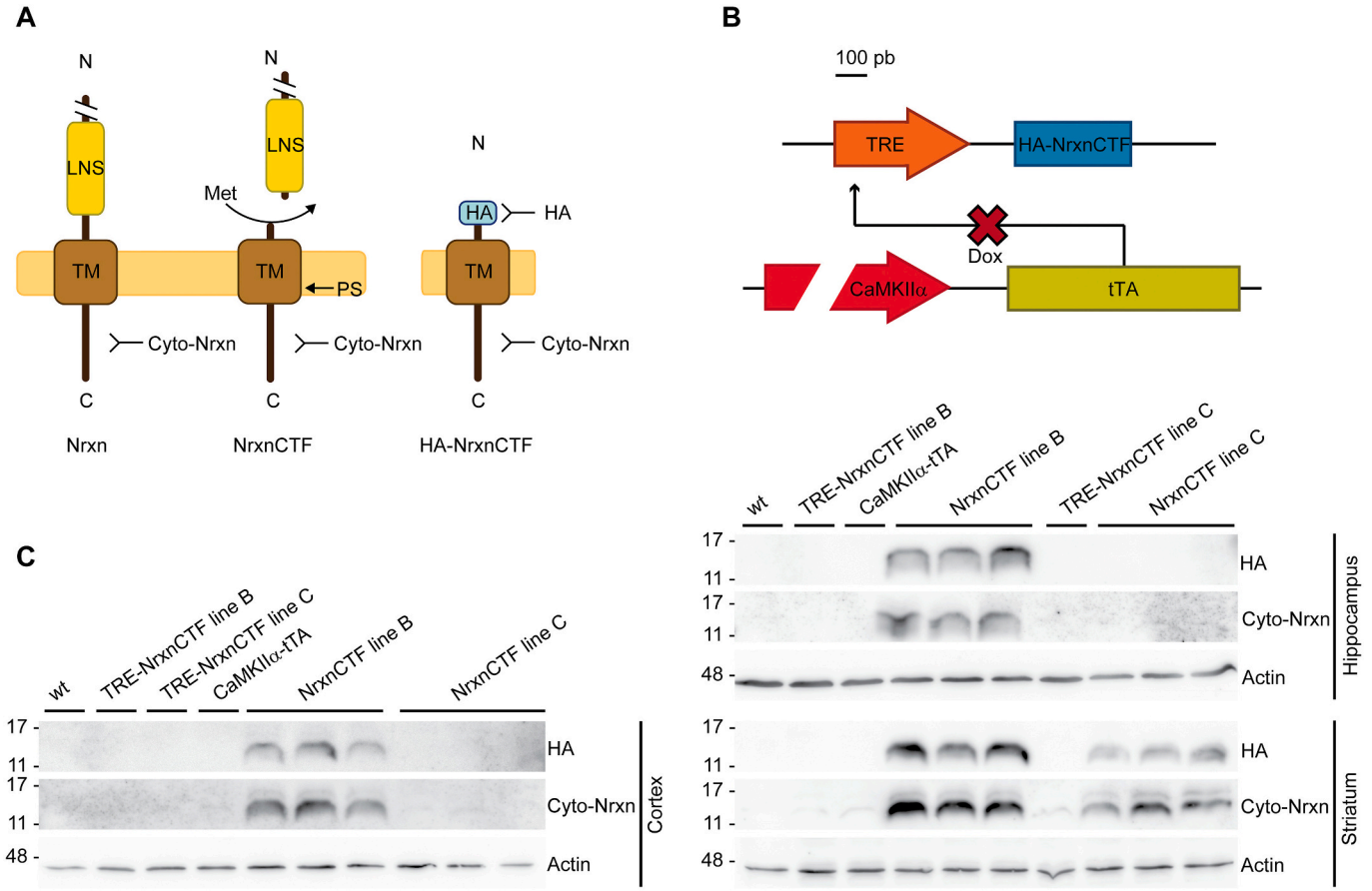

Fig. 1. Generation of NrxnCTF transgenic mice. A) Schematic drawings showing the proteolytic processing of Nrxns by metalloproteases and PS (left) and the HA-tagged NrxnCTF transgene used in this study (right). The regions recognized by the HA and the cyto-Nrxn antibodies are indicated. LNS, Laminin/Neurexin/Sex hormone binding-globulin domain; TM, transmembrane region. B) Representation showing the genetic approach for the expression of NrxnCTF in the forebrain. C) Expression of NrxnCTF in forebrain tissues of NrxnCTF mouse lines. NrxnCTF expression was analyzed in cortex, hippocampus and striatum by Western-blot experiments with HA and cyto-Neurexin antibodies, as indicated. Lysates from single transgenic CaMKIIα-tTA and TRE-NrxnCTF mouse lines were analyzed as additional controls.

the adult forebrain (Fig. 1). Mutagenesis analysis has previously showed that the last 85C-terminal residues of Nrxn1 represent the NrxnCTF substrate for PS/gamma-secretase (Servián-Morilla et al., 2018). Therefore, we generated a cDNA encoding NrxnCTF tagged at the N-terminus with an HA epitope to allow detection (Fig. 1A). The NrxnCTF construct was cloned under the control of the tetracycline-responsive element (TRE) (Fig. 1B). Two transgenic TRE-NrxnCTF mouse lines were obtained by nuclear injection, lines B and C. Transgene expression from the TRE promoter requires the co-expression in the same cells of the tetracycline transactivator (tTA). In PScKO mice, conditional deletion of PS genes in forebrain is achieved by the activity of a CaMKIIα promoter (Saura et al., 2004). Similarly, we chose a CaMKIIα-tTA allele to drive NrxnCTF expression in forebrain neurons (Mayford et al., 1996). Thus, we aimed at accumulating NrxnCTF with the same distribution than a loss of PS function would produce in forebrain neurons, but leaving PS/gamma-secretase activity unaltered (Fig. 1B). Double transgenic CaMKIIα-tTA;TRE-NrxnCTF mice (termed NrxnCTF mouse lines for simplicity) were born at the expected ratio. Expression of NrxnCTF was analyzed in lysates of forebrain regions by Western-blot experiments. The HA antibody recognized a major band of 14 kDa in lysates from hippocampus, cortex and striatum of NrxnCTF mice of line B (Fig. 1C). However, NrxnCTF was undetectable in the hippocampus and cortex of line C, and low expression levels were found at the striatum of the same line (Fig. 1C). A similar pattern of NrxnCTF expression was found in both mouse lines with an antibody that recognizes the common cytoplasmic tail of Nrxns, although a minor band of a lower mobility was more clearly detected in the transgenic mouse lines (Fig. 1C). In contrast, the HA antibody did not detect ectopic NrxnCTF expression in single transgenic mice (Fig. 1C), indicating the absolute requirement of the CaMKIIα-tTA driver for transgene expression. Notably, the expression pattern of NrxnCTF in line B recapitulates the accumulation of endogenous NrxnCTF in mice lacking PS function in the forebrain (Saura et al., 2011) (see below). Based on these data, we selected NrxnCTF mice from line B for further experiments.

3.2. Synaptic expression of NrxnCTF in adult forebrain

It has been reported that the CaMKIIα-tTA driver can promote transgene expression during pre- or early postnatal development (Nicholls et al., 2008; Roberts et al., 2009). This early expression might result in confounding effects when the impact of the transgene in the mature brain is upon evaluation (Rodgers et al., 2012), such in this study. We took advantage of the temporal-regulation provided by the Tet-off system to strictly limit the expression of NrxnCTF to adult forebrain. With this aim, we mated single transgenic CaMKIIα-tTA and TRE-NrxnCTF mice in the presence of diet with DOX and maintained the parental mice and their progeny in this diet until weaning, at postnatal day 30 (P30) (Fig. 2A). This time point matches the time at which PS gene deletion was reported in PScKO mice (Saura et al., 2004). As shown in Fig. 2B, this strategy results in the adult onset expression (>P30) of NrxnCTF at similar levels than untreated NrxnCTF mice.

Then, we interrogated if transgenic NrxnCTF recapitulates the expression at presynaptic terminals of synaptosome preparations previously described for the endogenously produced NrxnCTF in PScKO mice (Saura et al., 2011). In Western blot experiments of synaptosome preparations, transgenic NrxnCTF was found at synaptic fractions, where it concentrates at presynaptic, but not postsynaptic, terminals of cortex and hippocampus (Fig. 2C). The distribution of the synaptic markers PSD95 and SNAP25 within the post- and presynaptic fractions, respectively, confirmed the isolation protocol (Fig. 2C). These data indicate successful accumulation of NrxnCTF at presynaptic terminals of adult forebrain neurons once the formation of the synaptic circuitry is completed.

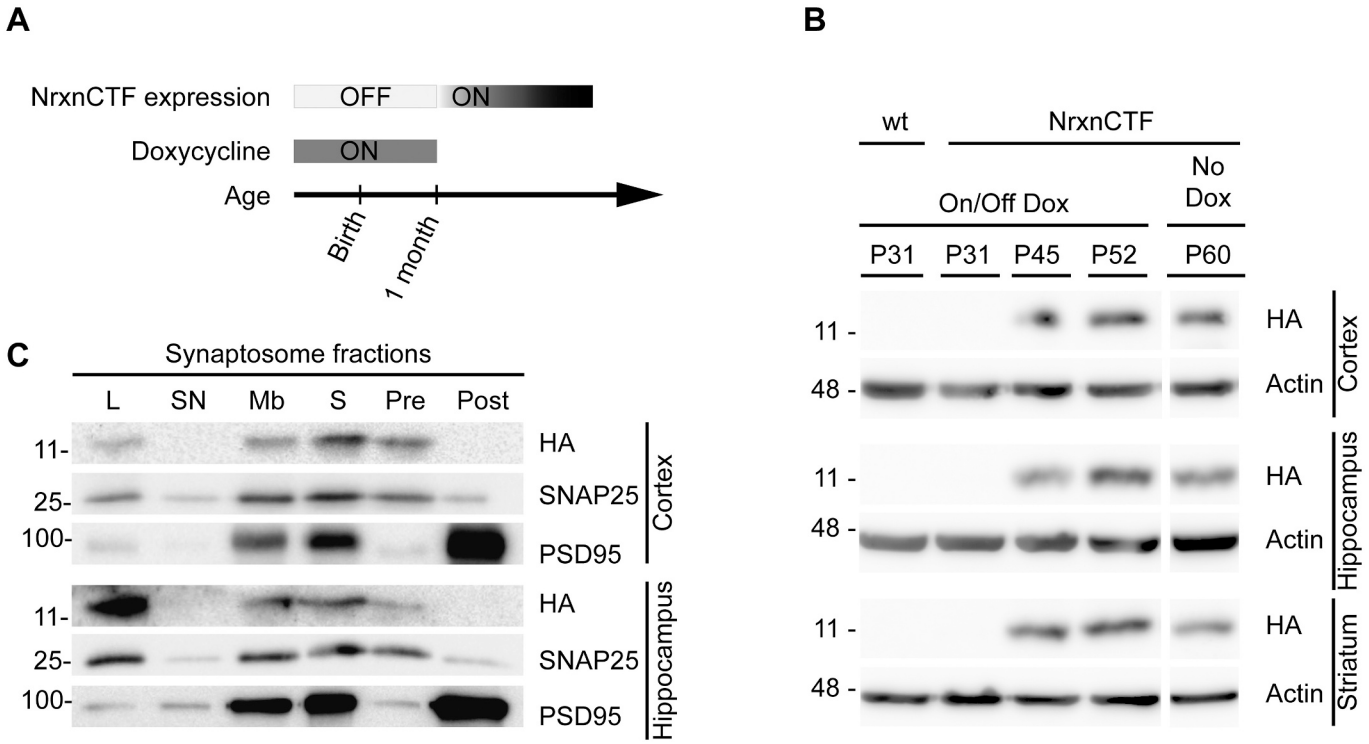

Fig. 2. Adult onset expression and distribution in synaptosome fractions from forebrain regions of NrxnCTF. A) Temporal control of NrxnCTF expression with DOX. B) Western-blot experiments showing NrxnCTF expression in adult forebrain of transgenic mice at different times after DOX removal at P30 (on/off). For comparison, NrxnCTF expression of untreated mice (No DOX) was analyzed for comparison. C) Synaptosome preparations from cortex and hippocampus of NrxnCTF mice were incubated with HA, SNAP25 and PSD95 antibodies, as shown. L, lysate; SN, supernatant; Mb, membrane; S, synaptosome; Pre, presynaptic fraction and Post, postsynaptic fraction. HA antibody detects the expression of NrxnCTF in presynaptic fractions of forebrain tissues.

3.3. Normal PS/gamma-secretase activity in NrxnCTF mouse

Our approach based on the selective accumulation of NrxnCTF aims at preserving PS levels and gamma/secretase function towards other substrates. To obtain experimental support for this hypothesis, we analyzed PS1 levels and the expression of representative PS substrates in lysates from NrxnCTF mice. To establish suitable comparisons for these experiments, we obtained mice with loss of PS function in adult forebrain neurons. For that, we mated PS1f/f;PS2−/− mice with transgenic CaMKIIα-CreERT2 mice to obtain PS1f/f;PS2−/−;CaMKIIα-CreERT2 mice. Then, Cre activity was induced with Tamoxifen at P30 to generate PScKO^{tam} mice. As a surrogate for the loss of PS function, we first analyzed the production of APP-CTF in PScKO^{tam} mice at different times after treatment with Tamoxifen. As shown in Fig. 3A, APP-CTF levels clearly increased in PScKO^{tam} mice from one to four months after treatment, indicating effective loss of PS function. Then, we selected for comparison PScKO^{tam} and NrxnCTF mice at 4.5 months, allowing for the same time after PS gene deletion and NrxnCTF expression, respectively. The levels of PS1 were reduced in the forebrain of PScKO^{tam} mice compared with controls, as expected (Fig. 3B, C). The remaining PS1 levels detected in PScKO^{tam} mice likely represent PS1 expression in CaMKIIα-promoter inactive neurons and in non-neuronal cells (Saura et al., 2004). By contrast, the expression of PS1 was not altered in NrxnCTF mice (Fig. 3B, C). Moreover, whereas N-Cadherin-CTF and APP-CTF accumulated in PScKO^{tam} mice, neither of these PS/gamma-secretase substrates showed accumulation in NrxnCTF mice. These data suggest that the levels and the proteolytic activity of the PS/gamma-secretase complex towards its substrates are not broadly affected by the expression of NrxnCTF.

As a further characterization of the mouse model, we decided to compare the expression of transgenic NrxnCTF with NrxnCTF produced in PScKO^{tam} mice. For that, Western blot experiments were performed with an antibody that recognizes the common cytoplasmic tail of Nrxns (Fig. 1). As expected, loss of PS function in PScKO^{tam} mice produced the accumulation of NrxnCTF in cortex and hippocampus (Fig. 3B, C). Importantly, the cyto-Nrxn antibody detected NrxnCTF proteins in

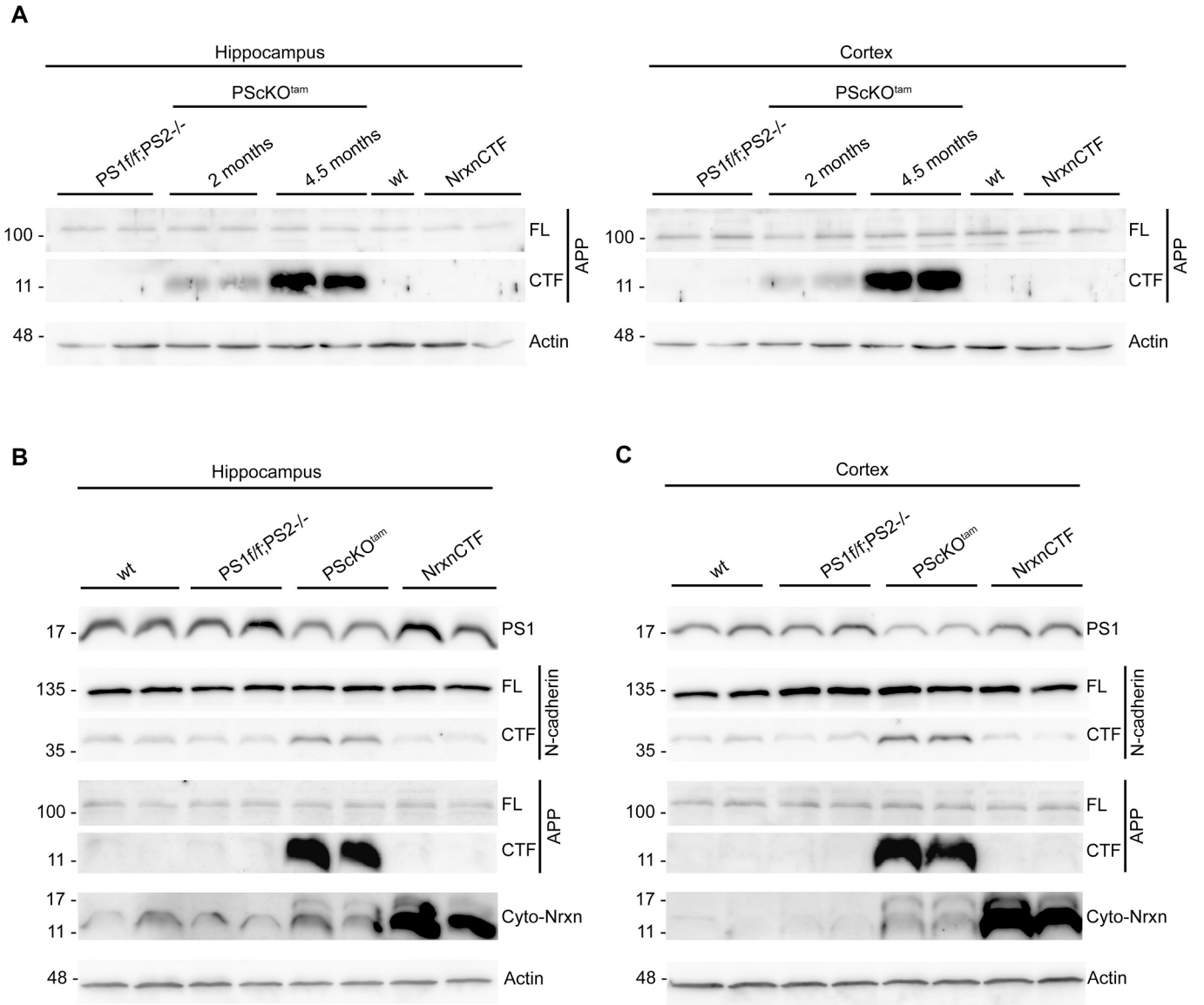

Fig. 3. Normal PS function in NrxnCTF mice. A) Accumulation of APP-CTF in hippocampal and cortical lysates of PScKO^{tam} mice at different times after PS deletion. NrxnCTF mice do not accumulate APP-CTF, as shown. B) Expression of PS1 and of selected PS/gamma-secretase substrates in PScKO^{tam} and NrxnCTF mice. Cortical and hippocampal lysates were analyzed by Western-blot with PS1, APP, N-Cadherin and cyto-Nrxn antibodies, as indicated. The cyto-Nrxn antibody recognizes the cytoplasmic tail of both endogenously produced NrxnCTF in PScKO^{tam} mice and NrxnCTF expressed in transgenic mice. Note that expression of PS1 or accumulation of gamma-secretase substrates are not affected in NrxnCTF mice.

transgenic mice with a similar pattern and tissue distribution than NrxnCTF accumulated in PScKO^{tam} mice (Fig. 3B, C). The level of NrxnCTF expression in transgenic mice was 4-5-fold higher than those of NrxnCTF in PScKO^{tam} mice, indicating moderate over-expression. A recent work failed to uncover accumulation of NrxnCTF in neurons lacking PS function (Barthet et al., 2018). While the reasons for these results are not known, detection of Nrxn proteins have been proved difficult and require proper immunological tools (Dean et al., 2003). Our experiments using different brain regions of mice lacking PS further confirm the accumulation of NrxnCTF. Collectively, the biochemical characterization indicate that NrxnCTF mice reproduce the impaired clearance of the Nrxn substrate for PS with the same tissue distribution and subcellular localization than a loss of PS function would generate in adult forebrain neurons, but leaving intact PS/gamma-secretase function towards other substrates.

3.4. Decreased stereotyped behavior and subtle social interaction deficits in NrxnCTF mice

NrxnCTF mice represent a suitable animal model to study the effects produced by a selective loss of PS/gamma-secretase function towards Nrxns. First, we conducted a battery of tests to uncover potential behavioral deficits. Within each test, NrxnCTF mice were compared with two types of controls, one control group comprised by wild-type and TRE-NrxnCTF mice and a second control group formed by CaMKIIα-tTA mice. These comparisons rule out any potential contribution that the CaMKIIα-tTA allele might cause in the phenotypes under study (Han et al., 2012). Locomotion was analyzed in the Open Field assay. Total distance as well as the distance travelled at the periphery and at the center were found similar in NrxnCTF mice and control groups (Fig. 4A), indicating that locomotion is not affected in NrxnCTF mice.

Besides memory problems, neuropsychiatric features are often

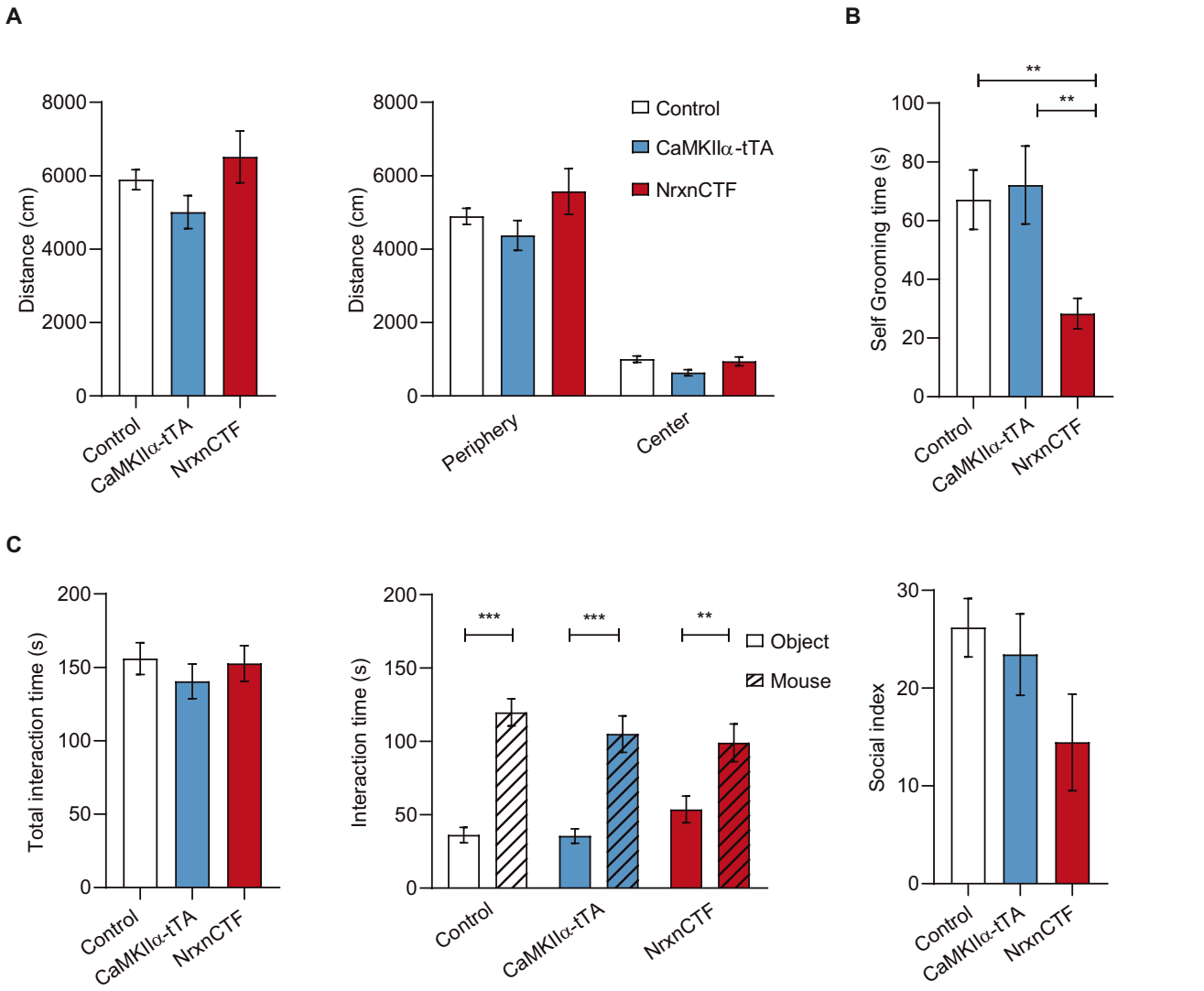

Fig. 4. Locomotion, repetitive behavior and social interaction in NrxnCTF mice. A) Open field assay. Total distance and distance travelled per area are shown. Total distance: control 5893 ± 273.7; CaMKIIα-tTA 5008 ± 450.4; NrxnCTF 6509 ± 705.3. Distance at the periphery: control 4892 ± 218.2; CaMKIIα-tTA 4374 ± 406.9; NrxnCTF 5569 ± 625.2. Distance at the center: control 1001 ± 86.29; CaMKIIα-tTA 634.1 ± 83.31; NrxnCTF 940.5 ± 120. Distance in cm. Control, $n = 29$; CaMKIIα-tTA, $n = 15$; NrxnCTF, $n = 24$. B) Reduced self-grooming time in NrxnCTF mice compared with control groups. Control 67.10 ± 10.09; CaMKIIα-tTA 72.10 ± 13.29; NrxnCTF 28.31 ± 5.19. Time in s. Control, $n = 28$; CaMKIIα-tTA, $n = 14$; NrxnCTF, n = 24. C) Social interaction in the three-chamber test. Graphs show total time spent in interaction with the mouse and the object (left), time interacting with the mouse or the object (center) and social index (left). Total interaction time: control 156.0 ± 10.77; CaMKIIα-tTA 140.5 ± 11.86; NrxnCTF 152,7 ± 12,13. Time interacting with the object: control 36.19 ± 5.20; CaMKIIα-tTA 35.51 ± 4.92; NrxnCTF 53.61 ± 9.08; time interacting with the mouse: control 119.8 ± 9.26; CaMKIIα-tTA 105.0 ± 12.42; NrxnCTF 99.05 ± 12.85. Time in s. Social index: control 26.18 ± 2.99; CaMKIIα-tTA 23.43 ± 4.15; NrxnCTF 14.46 ± 4.93. Control, $n = 17$; CaMKIIα-tTA, $n = 12$; NrxnCTF, $n = 12$. ** $p < 0.01$, *** $p < 0.001$.

associated with AD, including altered stereotypic behavior and social apathy (Bozeat et al., 2000; Cerejeira et al., 2012; Prioni et al., 2012). Repetitive behavior was studied in the self-grooming assay in which the time dedicated to perform a stereotyped sequence of movements is quantified (Fig. 4B). Interestingly, self-grooming time in NrxnCTF mice was decreased by over 50% as compared with control and CaMKIIα-tTA mice (Fig. 4B). The number of self-grooming bouts was similar in the three groups (control: 3.71 ± 0.38; CaMKIIα-tTA: 4.42 ± 0.74; NrxnCTF: 3.41 ± 0.32; $p > 0,05$), but NrxnCTF mice showed shorter duration of self-grooming events (control: 19.64 ± 3.09; CaMKIIα-tTA: 18.76 ± 3.70; NrxnCTF: 9.02 ± 1.71; $p < 0.01$; time in s). Social interaction was evaluated in the three-chamber test (Fig. 4C). In this assay, the tested mouse is placed in a middle chamber and the time interacting with an inanimate stimulus or with a mouse located in side chambers is analyzed. Total interaction time with either of the two stimuli was found similar in the three animal groups (Fig. 4C). Furthermore, NrxnCTF mice showed preferential interaction with the mouse compared with the object, although the average time interacting with the object slightly increased in NrxnCTF mice as compared with control groups, without reaching statistical significance (Fig. 4C). This trend towards decreased social interaction in NrxnCTF mice was detected with the social index, which measures the percentage of time that each animal differentially interacts with the mouse (Fig. 4C). These findings indicate that expression of NrxnCTF in adult forebrain produces decreased stereotyped behavior and subtle deficits in social interaction.

3.5. Normal recognition memory and spatial memory in NrxnCTF mice

Memory deficit is a core symptom in AD and mouse models lacking PS expression. Therefore, we analyzed the performance of NrxnCTF mice in several memory assays. The novel object recognition test evaluates the innate preference of a mouse to interact with a novel object

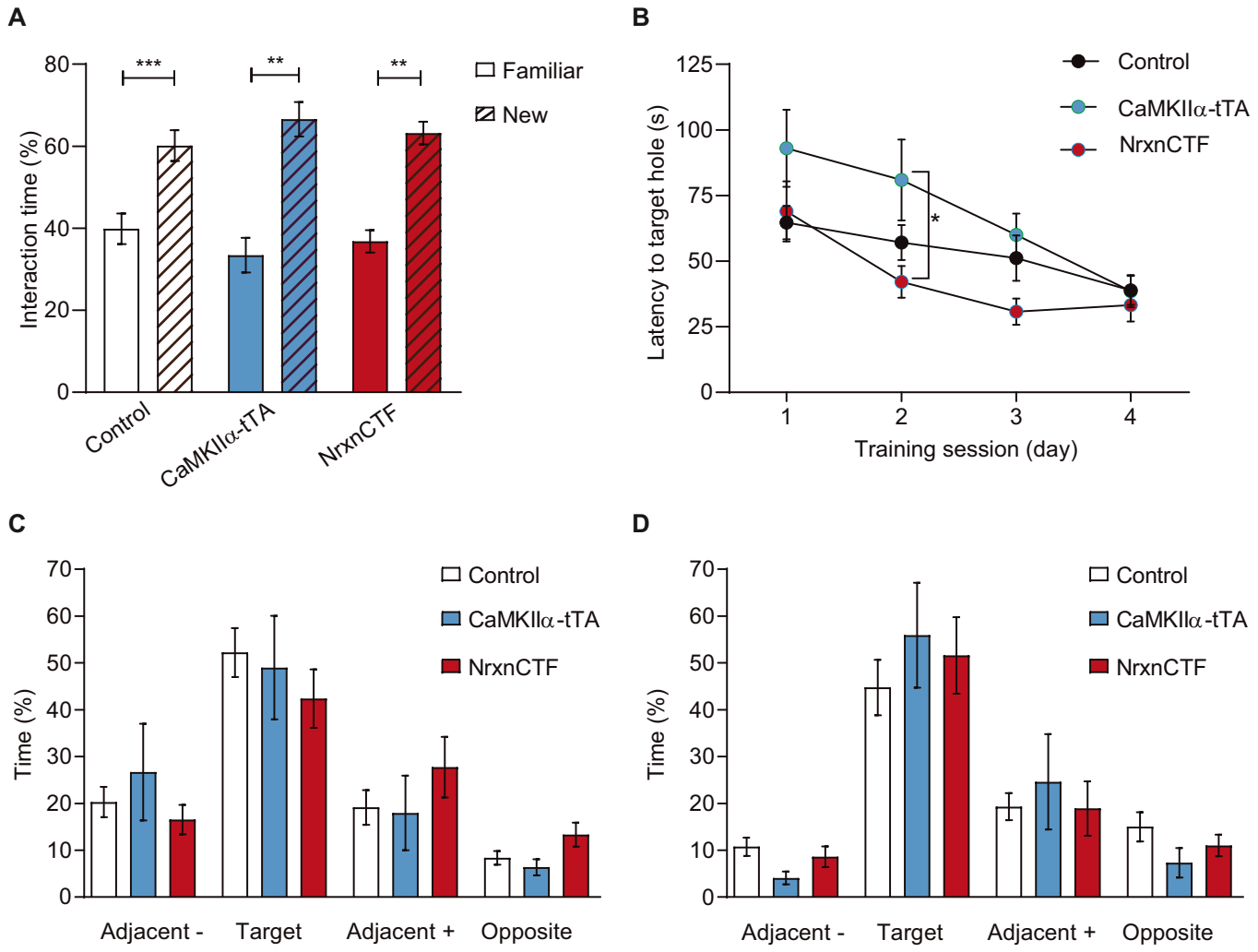

Fig. 5. Normal spatial and recognition memories in NrxnCTF mice. A) Novel object recognition. Similar average time interacting with the familiar or novel object in NrxnCTF mice compared with control groups. Control, familiar object 39.86 ± 3.75%, novel object 60.14 ± 3.75%; CaMKIIα-tTA, familiar object 33.42 ± 4.22%, novel object 66.58 ± 4.22%; NrxnCTF, familiar object 36.79 ± 2.74%, novel object 63.21 ± 2.74%. Control, n = 17; CaMKIIα-tTA, $n = 5$; NrxnCTF, $n = 11$. B-D) Barnes maze test. B) Time latency to find the escape hole during the four training sessions. Control 64.72 ± 6,35, 57.11 ± 6.73, 51.19 ± 8.71, 38.91 ± 5.54; CaMKIIα-tTA 93.00 ± 14.65, 80.9 ± 15.41, 59.97 ± 8.16, 38.53 ± 6.15; NrxnCTF 68.94 ± 11.47, 42.12 ± 6.07, 30.79 ± 5.06, 33.28 ± 6.28. Time in s. C) Percentage of time spent in quadrant one day after training. Adjacent -, control 20.28 ± 3.23%, CaMKIIα-tTA 26.69 ± 10.34%, NrxnCTF 16.54 ± 3.12%; target, control 52.22 ± 5.22%, CaMKIIα-tTA 48.99 ± 11.06%, NrxnCTF 42.39 ± 6.23%; adjacent +, control 19.13 ± 3.68%, CaMKIIα-tTA 17.96 ± 7.96%, NrxnCTF 27.76 ± 6.46%; opposite, control: 8.36 ± 1.47%, CaMKIIα-tTA: 6.36 ± 1.74%, NrxnCTF 13.32 ± 2.55%. D) Percentage of time spent in quadrant eight days after training. Adjacent-, control 10.74 ± 1.97%, CaMKIIα-tTA 4.08 ± 1.35%, NrxnCTF 8.60 ± 2.19%; target, control 44.74 ± 5.89%, CaMKIIα-tTA 55.90 ± 11.20%, NrxnCTF 51.57 ± 8.16%; adjacent +, control 19.29 ± 2.89%, CaMKIIα-tTA 24.60 ± 10.19%, NrxnCTF 18.91 ± 5.82%; opposite, control 14.99 ± 3.13%, CaMKIIα-tTA 7.31 ± 3.14%, NrxnCTF 11.02 ± 2.32%. Control, $n = 18$; CaMKIIα-tTA, n = 12; NrxnCTF, n = 12. * $p < 0.05$, ** $p < 0.01$, *** $p < 0.001$.

presented along a familiar one. NrxnCTF mice showed no differences with control groups in the preferential interaction with the novel object (Fig. 5A). Spatial memory was studied in the Barnes Maze. In this test, mice are exposed to a round open space delimited by holes in the periphery, where only one of them is an escape hole. After repeated sessions, mice learn to find shelter in the escape hole using spatial cues placed in the periphery. During learning, NrxnCTF mice and control groups spent similar time to find the escape hole in the initial and the final fourth session, although the escape time in the second and third sessions was reduced in NrxnCTF mice (Fig. 5B). After learning, the escape hole is closed and spatial memory is evaluated one and eight days later. At both time points, NrxnCTF mice showed no differences with control groups in the time spent in the target quadrant (Fig. 5C, D). These data indicate that recognition and spatial memories are not affected in NrxnCTF mice.

3.6. Decreased fear-conditioning memory in NrxnCTF mice

We evaluated fear-memory, a form of associative learning depending on the amygdala and hippocampus (Kim and Fanselow, 1992; Phillips and LeDoux, 1992). In the fear-conditioning assay, mice learn by repetition to associate a neutral stimulus, a tone (the conditioned stimulus, CS), with a behavioral significant stimulus co-terminating with the CS, a mild electric shock (the unconditioned stimulus, US). NrxnCTF mice showed no significant differences with controls during conditioning evaluated as the freezing time during CS-US pairing (Fig. 6A). Contextual- and auditory-fear memory was evaluated one day after CS-US pairing. NrxnCTF mice showed similar freezing time than controls when exposed to the arena where CS-US stimuli were paired, indicating that NrxnCTF mice can evoke a freezing response (Fig. 6B). However, NrxnCTF mice showed reduced freezing time to the tone presented in a new arena (Fig. 6C). The reduced CS-dependent memory of NrxnCTF mice was not due to an effect of the CaMKIIα-tTA allele (Fig. 6C). These data indicate that expression of NrxnCTF in mature forebrain decreases associative fear memory.

3.7. Altered short term synaptic plasticity at mPFC-BLA synapses of alert behaving NrxnCTF mice

Cortical inputs from the mPFC regulate the expression of fear memories stored in the amygdala (Burgos-Robles et al., 2009; Corcoran and Quirk, 2007; Sotres-Bayon and Quirk, 2010). The presynaptic expression of NrxnCTF by cortical neurons along with the decrease in fear memory in NrxnCTF mice, pointed at mPFC-BLA synapses as an appropriate pathway to uncover potential synaptic effects caused by NrxnCTF. Control and NrxnCTF mice (n = 10 mice/group) were

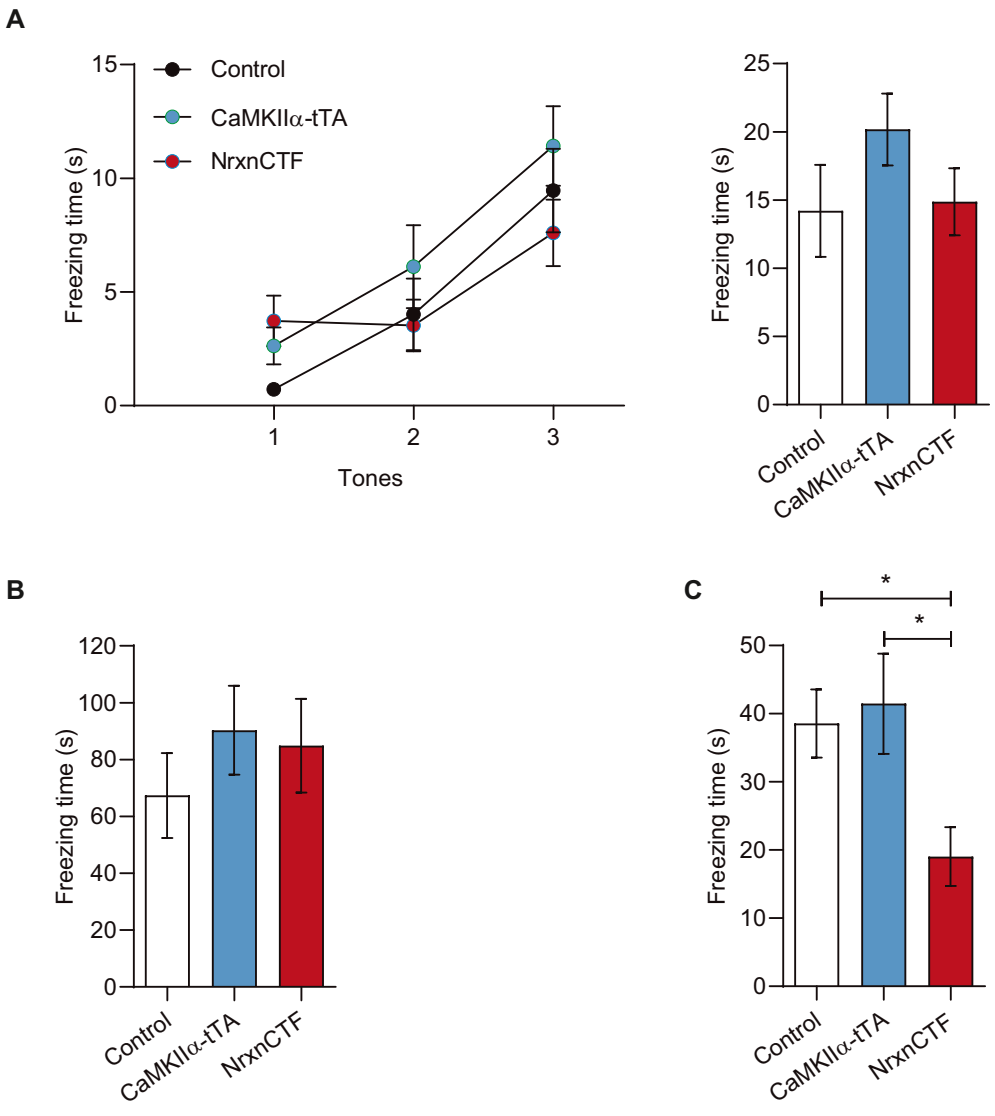

Fig. 6. Decreased fear memory in NrxnCTF mice. A) Freezing time during the conditioning session. Control 14.20 ± 3.37; CaMKIIα-tTA 20.17 ± 2.63; NrxnCTF 14.87 ± 2.45. B) Freezing time in the context. Control 67.35 ± 14.98; CaMKIIα-tTA 90.30 ± 15.66; NrxnCTF 84.85 ± 16.47. C) Decreased freezing response during tone presentation in NrxnCTF mice. Control 38.56 ± 4.99; CaMKIIα-tTA: 41.46 ± 7.35; NrxnCTF 19.04 ± 4.30. Control, n = 19; CaMKIIα-tTA, n = 13; NrxnCTF, n = 14. Time in s. * $p < 0.05$.

implanted with stimulating and recording electrodes in mPFC and BLA, respectively, for chronic fEPSP recordings (Fig. 7A, B). Wild-type and single transgenic mice were included in the same control group as no differential effects were detected in the previous experiments. The correct location of the electrodes was analyzed by histological procedures at the end of the recording sessions (Fig. 7C). The short latency (< 4 ms) and negative profiles of evoked fEPSPs (Fig. 8B) suggest that we were recording monosynaptic excitatory field responses evoked at mPFC-BLA synapses (Arruda-Carvalho and Clem, 2014; Hübner et al., 2014).

First, we checked the general functional properties of the mPFC-BLA synapses by evoking fEPSP with paired-pulse (40 ms inter-stimulus) stimulation of increasing intensities (0.02–0.4 mA). Both control and NrxnCTF animals presented input/output curves with similar sigmoid-like profiles (Fig. 8A), suggesting that basal functional properties of mPFC-BLA synapses are not affected in NrxnCTF mice.

To analyze short-term synaptic plasticity, we performed a paired-pulse ratio (PPR) test at different inter-stimulus intervals (10, 20, 40, 100, 200 and 500 ms; $F_{(5,45)} = 6.718$; $P < 0.001$). mPFC-BLA synapses of control mice presented a paired-pulse facilitation (PPF) with maximum facilitation at 20 ms (Fig. 8B). Interestingly, NrxnCTF mice lack facilitation at 20 ms and instead presented facilitation at the 100 ms inter-stimulus interval (Fig. 8B). These data indicate that accumulation of NrxnCTF delays the optimal range for synaptic facilitation at mPFC-BLA synapses.

Last, we evoked LTP by the application of HFS in mPFC and recording of the effects in the BLA. LTP evolution in the BLA was recorded for 1 h the first day and for 30 min the three following days. As a result, both control ($F_{(32, 252)} = 8.555$; $P < 0.001$) and NrxnCTF ($F_{(32, 226)} = 4.255$; $P < 0.001$) groups seemed to have significant LTP, especially in day one, that decreased in the following days (Fig. 9A). Nevertheless, there were no statistically significant differences between groups or pulses (1st or 2nd) (Fig. 9A). Interestingly, we noticed a difference in the PPF evoked by LTP in the two groups (Fig. 9B). The relationship between 2nd and 1st pulses has been reported as an indicator for the presence of a presynaptic component of LTP (Madroñal et al., 2009). We calculated PPR following LTP induction with the following equation: (2nd pulse/1st pulse) x 100; and obtained the regression line for both groups (Fig. 9B). Control mice had a steeper (slope: 0.6143) regression line than NrxnCTF mice (slope: 0.3863) following LTP induction (equations and statistical values are shown in Fig. 9B). This suggests that NrxnCTF mice have a certain reduction in the presynaptic facilitation induced by the HFS protocol. Overall, the data collected from behaving mice in basal conditions and following the application of HFS indicate that accumulation of NrxnCTF impairs short-term synaptic plasticity.

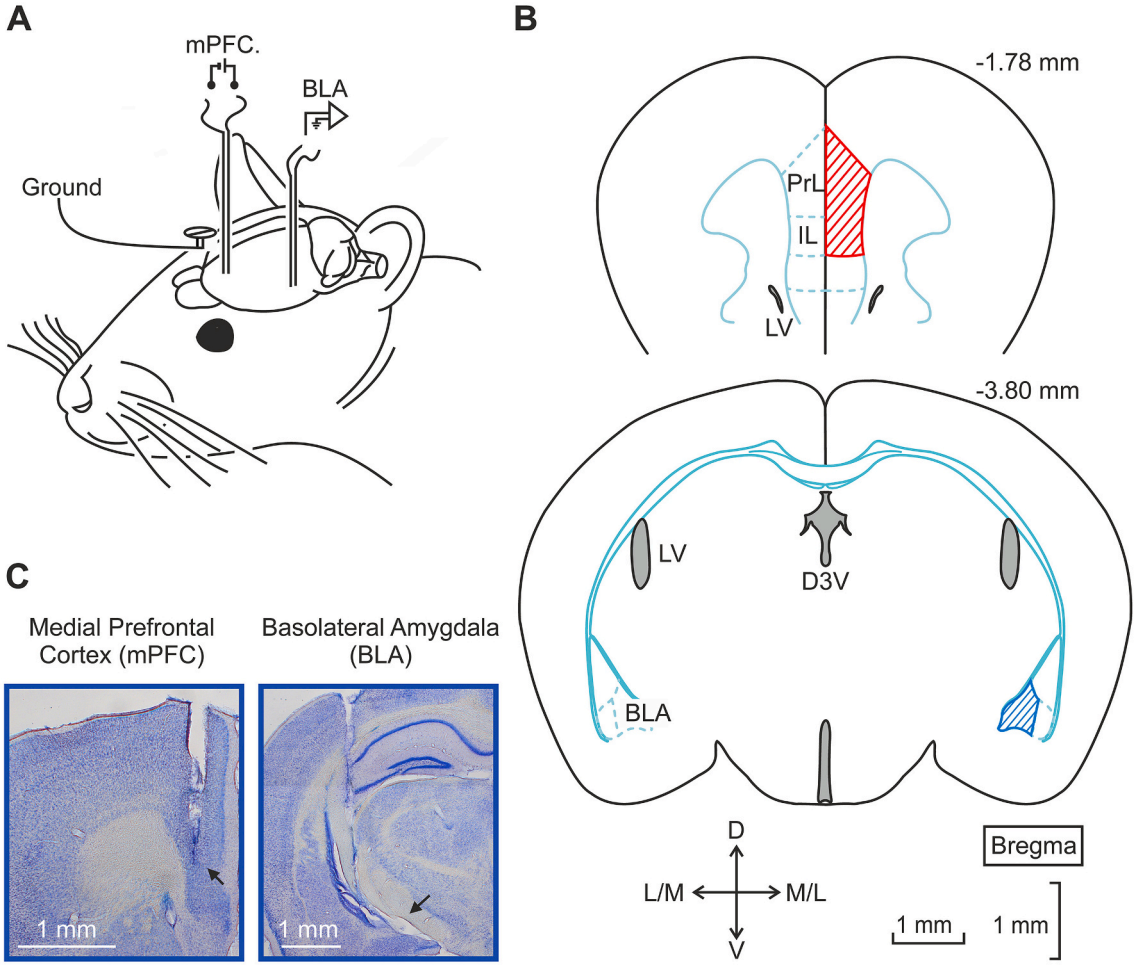

Fig. 7. Electrodes implantation. A) A bipolar stimulation electrode was implanted in the mPFC, and recording electrode was implanted in the BLA of the same hemisphere. A screw was fixed to the skull, serving as a ground. B) An illustration of two coronal slices from the mouse brain where the shaded areas indicate the location of the electrodes: red stands for the mPFC (up) and blue stands for the BLA (down). Diagrams and coordinates correspond to Franklin and Paxinos (2007). C) Representative micrographs of the electrode scar in mPFC (left) and BLA (right). (For interpretation of the references to colour in this figure legend, the reader is referred to the web version of this article.)

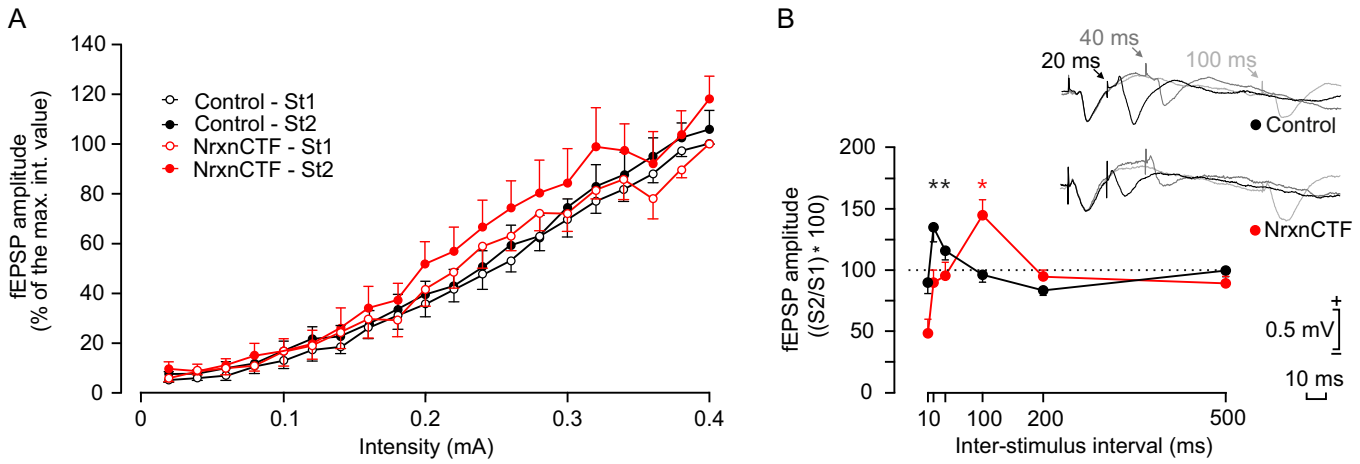

Fig. 8. Input/output curves and PPF evoked at mPFC-BLA synapses in control and NrxnCTF mice. A) Input/output (I/O) curves from control (black) and NrxnCTF (red) mice for both 1st (open circles) and 2nd (closed circles) pulses. This test reported a similar progress of the fEPSP amplitude along increasing intensities (from 0.02 mA to 0.4 mA in intervals of 0.02 mA) for both groups. Data are normalized as the percentage of the amplitude corresponding to the maximum intensity. Every point of each animal ($n \geq 7$ per group) represents the mean value of 10 pulses. B) At the top are illustrated examples of fEPSP recordings from control and NrxnCTF mice during the PPF test, representative of the 3 time-intervals of maximum facilitation (20, 40, and 100 ms). Results of the PPF test for control (black) and NrxnCTF mice (red) are shown below. Data are represented as the ratio 2nd pulse/1st pulse of the fEPSP amplitude multiplied by 100, along increasing interstimulus intervals (10, 20, 40, 100, 200, and 500 ms). Every point of each animal ($n = 10$ per group) represents the mean value of 10 stimuli. * $p < 0.05$ in comparison with the values at 500 ms —the most similar to baseline values. (For interpretation of the references to colour in this figure legend, the reader is referred to the web version of this article.)

4. Discussion

PS function is crucial to maintain normal synaptic function and memory in mature brain. Causative mutations in *PSEN* genes lead to fAD by a loss of function mechanism, highlighting the need for the identification of PS/gamma-secretase substrates of functional significance. Loss of PS function is commonly analyzed in approaches that result in the broad inhibition of the gamma-secretase proteolytic activity towards the full repertoire of substrates, limiting the functional validation of individual candidates. By using adequate expression drivers, we recreated the accumulation of the Nrxn substrate for PS in adult forebrain neurons without affecting PS/gamma-secretase activity towards other substrates. We showed that NrxnCTF transgenic mice recapitulate the tissue distribution and the subcellular location of endogenously produced NrxnCTF caused by a loss of PS activity in the same forebrain regions. Importantly, NrxnCTF mice presented behavioral deficits, including decreased fear memory. Electrophysiological recordings at the mPFC-BLA synapses of alert behaving animals uncovered impaired presynaptic facilitation processes in NrxnCTF mice. Together, these data indicate that the impaired clearance of NrxnCTF may play a role in memory and synaptic plasticity deficits caused by a loss of PS function in fAD.

The proteolytic processing of Nrxns has the ability to modulate the function of the synapse and, when altered, affect synapse physiology. The cleavage of the extracellular domain of Nrxn isoforms can regulate specific interactions with synaptic ligands (Peixoto et al., 2012; Suzuki et al., 2012), whereas the proteolytic clearing of the resulting NrxnCTF can avoid undesired interactions at the synapse (Servián-Morilla et al., 2018). Currently, it is unknown if a specific subset of Nrxns participate in the generation of NrxnCTF *in vivo*. However, the cleavage of the specific ectodomain of Nrxn isoforms produces a common NrxnCTF because Nrxns share the transmembrane and cytoplasmic regions (Saura et al., 2011; Servián-Morilla et al., 2018). Based on these findings, we generated a transgene encoding the C-terminal residues of *Nrxn1* downstream of the ectodomain cleavage site that recreates the common NrxnCTF. We put special effort to direct the expression of NrxnCTF within a meaningful neuronal framework. The function of PS in mature brain has been extensively evaluated in PScKO mice, in which Cre-dependent deletion of PS genes was achieved in forebrain neurons by means of a CaMKIIα promoter (Saura et al., 2004). Similarly, we directed the expression of NrxnCTF to forebrain neurons by using an inducible system driven by a CaMKIIα promoter. Furthermore, the selection of an inducible system offers precise temporal control for the expression onset, which we initiated in adulthood ($P > 30$). We also generated PScKO^{tam} mice in which inhibition of PS genes in forebrain neurons was initiated at P30, recreating the loss of PS genes reported in PScKO mice (Saura et al., 2004). By comparing NrxnCTF produced in transgenic mice and conditional PScKO^{tam} mice, we showed that expression of transgenic NrxnCTF showed a tissue distribution in forebrain regions similar to the endogenously produced NrxnCTF in PScKO^{tam} mice. Importantly, NrxnCTF mice presents normal PS1 levels and activity towards other gamma-secretase substrates, which opposed to the lack of PS expression and accumulation of substrates that occurs in PScKO^{tam} mice. Moreover, NrxnCTF concentrates at presynaptic terminals of synaptosome preparations of transgenic mice, showing the same subcellular distribution previously reported for NrxnCTF in PScKO mice (Saura et al., 2011). Thus, the biochemical characterization validated the selective expression of a single PS/gamma-secretase substrate, NrxnCTF, in the mature forebrain.

Functional characterization of NrxnCTF mice identified deficits in selected behavioral outcomes. NrxnCTF mice showed decreased repetitive behavior in the self-grooming assay, mainly due to shorter duration of self-grooming events. In the three-chamber test, NrxnCTF mice preferentially interacted with a mouse over an object as controls, although NrxnCTF mice showed a trend towards decreased social interaction. Mutations and deletions in *NRXN1* gene have been found repeatedly in patients of neurodevelopmental disorders, including autism and schizophrenia (Camacho-Garcia et al., 2013; Camacho-Garcia et al., 2012; Guilmatre et al., 2009; Rujescu et al., 2009; Szatmari et al., 2007). Interestingly, the performance of NrxnCTF mice in the self-grooming assay and in the three-chamber test oppose to the increased repetitive behavior and impaired social interaction found in an autism-associated mouse model expressing a Nrxn1 mutant thought to work in a dominant-negative way (Rabaneda et al., 2014). The expression of both Nrxn transgenes in these two mouse models was achieved using the same CaMKIIα-tTA driver. These data suggest that the defects caused by NrxnCTF are not simply due to a loss of Nrxn function, but rather to a

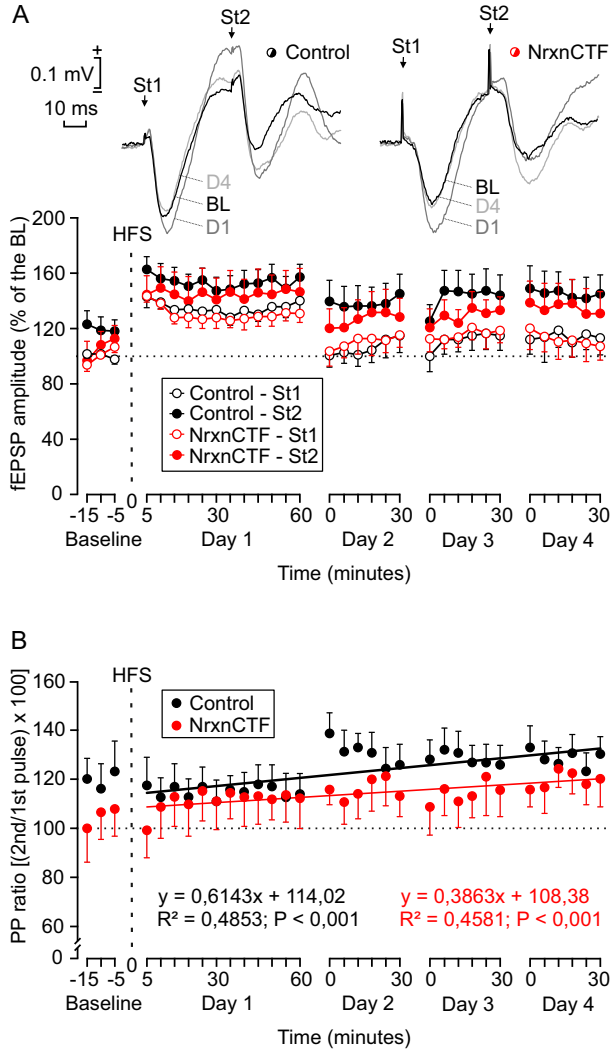

Fig. 9. Differences in LTP evoked at mPFC-BLA synapses in control and NrxnCTF mice. A) At the top are illustrated representative examples of fEPSP recordings collected during LTP induction in control (left) and NrxnCTF (right) mice. Arrows point to 1st and 2nd stimuli. BL: baseline, D1 and D4: 1st and 4th day after the HFS session. The LTP evoked in the BLA after the HFS applied to the mPFC is represented below. Black symbols stand for control mice and red ones stand for NrxnCTF mice. The effects of 1st (circles) and 2nd (dots) pulses are plotted. LTP effect was quantified during 4 days after the induction and is shown as a percentage of the 1st pulse of baseline amplitude. Every point of each animal ($n = 9$ animals/ group) represents the mean value of 15 pulses for each 5 min interval. St1: 1st stimulus and St2: 2nd stimulus. B) Linear regression analysis following LTP. The control group (black dots and line) presented a linear regression line with a stepper slope (0.6143 *vs.* 0.3863) than in the NrxnCTF group (red dots and line). (For interpretation of the references to colour in this figure legend, the reader is referred to the web version of this article.)

gain-of-function mechanism caused by the impaired clearance of NrxnCTF.

Fear-conditioning memory was decreased in NrxnCTF mice. The specific defects in tone-dependent fear memory suggested that expression of NrxnCTF produces a malfunctioning of synaptic circuits relevant for this form of associative memory. Based on the presynaptic expression of NrxnCTF by cortical excitatory neurons and the crucial role of mPFC excitatory inputs to BLA in fear expression (Burgos-Robles et al., 2009; Corcoran and Quirk, 2007), we reasoned that mPFC-BLA synapses provide an informative framework to search for synaptic defects caused by NrxnCTF. Field EPSP recordings at mPFC-BLA synapses of alert behaving mice revealed specific defects at PPF in NrxnCTF mice. PPF is a form of short-term synaptic plasticity that is used as an indirect measurement of changes in the probability of release of neurotransmitter at the presynaptic terminal (Lauri et al., 2007; Madroñal et al., 2009; Zucker and Regehr, 2002). It is assumed that presynaptic components of LTP could modify the PPF ratio by affecting the mechanism of transmitter release (Andreescu et al., 2007). In contrast, the post-synaptic form of the LTP will not affect the PPF ratio, because those changes are assumed to take place at the post-synaptic site (Andreescu et al., 2007; Madroñal et al., 2009; Zucker and Regehr, 2002).

In control mice, mPFC-BLA synapses showed maximum facilitation at 20 ms inter-stimulus interval. However, NrxnCTF mice failed to facilitate at this short interval and instead presented facilitation at 100 ms. Facilitation is mediated by presynaptic changes in residual calcium following a previous closely-spaced stimulus (Katz and Miledi, 1968; Thomson, 2000; Zucker and Regehr, 2002). Notably, we have previously found that expression of NrxnCTF decreases activity-dependent calcium influx and neurotransmitter release in cultured neurons (Servián-Morilla et al., 2018), pointing at altered calcium signaling as a potential mechanism affected in NrxnCTF mice. Analysis of PPR induced by HFS further supported a deleterious role of NrxnCTF in short-term synaptic plasticity. We found that HFS produced LTP in mPFC-BLA synapses of control mice that peaked at day one and decayed in the following days. PPF did not change during LTP expression, suggesting a postsynaptic component, but PPF increased following LTP, indicating a dynamic change in the probability of release. The induction of LTP at mPFC-BLA synapses of NrxnCTF mice was found of similar magnitude and duration than controls. However, the increase in PPF following LTP was reduced in NrxnCTF mice as compared with controls. Interestingly, synaptic facilitation transiently increases in the hippocampus of behaving mice during the acquisition of an associative learning paradigm (Madroñal et al., 2009). In cortical afferents to BLA, modification of release probability underlies the expression of homosynaptic and heterosynaptic LTP in slice preparations (Huang and Kandel, 1998; Humeau et al., 2003). These data suggest that the presynaptic accumulation of NrxnCTF might alter a mechanism important for dynamic changes in release probability and synaptic facilitation related to associative memory.

When comparing the phenotype of NrxnCTF mice with the behavioral and synaptic alterations in PScKO mice, several points arise. The impaired fear memory of NrxnCTF mice resembles the deficits found in tone-dependent fear memory of PScKO mice, but spatial and recognition memory are only affected in PScKO mice and spared in NrxnCTF mice (Cao et al., 2018; Feng et al., 2004; Saura et al., 2004). It is not currently known if these differences arise from a role of NrxnCTF exclusively affecting circuits important for fear memory or from differences in the experimental conditions. As an example, spatial memory has been explored in PScKO mice using the Morris Water Maze, a more stressful test for mice than the Barnes Maze used in this study (Harrison et al., 2009). Furthermore, ongoing neurodegeneration can likely affect the performance of memory tests when analyzed in aged mice (Feng et al., 2004). At the synaptic level, PS activity is essential to regulate short-term plasticity acting through several mechanisms that depend on the identity of the synapse under study. Deletion of PS1/2 impairs synaptic facilitation and short-term plasticity in hippocampal neurons through a presynaptic mechanism that depends on calcium release from the endoplasmic reticulum at CA3-CA1 synapses or from the mitochondria at dentate gyrus (DG)-CA3 synapses (Lee et al., 2017; Zhang et al., 2009). In addition, PS1/2 genes in hippocampal DG neurons are required to maintain the levels of the calcium sensor synaptotagmin-7, a presynaptic protein important for synaptic facilitation (Barthet et al., 2018). Genetic deletion of APP in DG neurons lacking PS1 gene rescues synaptotagmin-7 levels and normalizes short-term plasticity at DG-CA3 synapses, suggesting a functional contribution of APP-CTF (or APP) in the short-term plasticity defects caused by inactivation of PS (Barthet et al., 2018). The synaptic mechanism underlying impaired fear memory in PScKO mice is not known. Our findings from behaving mice

indicating that NrxnCTF impairs synaptic facilitation at mPFC-BLA synapses are consistent with a broad role of PS in the regulation of short-term plasticity in AD (Barthet and Mulle, 2020). It remains to be investigated whether NrxnCTF affects short-term plasticity in other forebrain regions where it accumulates upon inactivation of PS genes, such as the hippocampus.

Collectively, our study demonstrates that failure in the synaptic clearance of NrxnCTF results in defects in short-term synaptic plasticity and associative memory. Because defects in synaptic facilitation and fear-conditioning memory are early effects caused by the inactivation of PS (Saura et al., 2004), the data shown here point at NrxnCTF as a relevant mediator related to the inhibition of PS function. The discovery of new players with a functional impact in the loss of PS function may represent an important step in AD. Furthermore, it is unlikely that a single PS/gamma-secretase substrate will explain the plethora of deficits caused by a loss of PS function, highlighting the participation of multiple mediators with functional relevance at specific roles. Our data suggest that NrxnCTF is a novel player that can participate in the synaptic and memory deficits associated with a loss of PS function in AD.

Funding statement

This work was funded by a grant from Ministerio de Ciencia, Innovación y Universidades (RTI2018-101886-B-100) to FGS and AM-M, Junta de Andalucía (PY18-823) to JMG-D, and co-funded by ERDF. ACS-H was the recipient of a fellowship from Junta de Andalucía (P11-CVI-7599). FAA was the recipient of a fellowship from Ministerio de Economía, Industria y Competitividad (BES-2016-076579). CM-C was the recipient of a Garantía Juvenil contract from Universidad de Sevilla.

Declaration of Competing Interest

None of the authors declare any conflict of interests.

Acknowledgments

The authors would like to thank Dr. J. Shen for providing fPS1/fPS1; PS2 -/- mice; German Cancer Research Center (DKFZ) and Institute of Genetics and Molecular and Cellular Biology (IGBMC) for providing CaMKII-Cre-ERT2 transgenic mice; Dr. Rafael Fernández-Chacón for critical advice and help with mouse colonies; Drs. María Luz Montesinos and Itziar Benito for advice in the Barnes maze; Dr. Francisco Morón, from the Genomics and Sequencing facility at IBiS, and Dr. Francisco Martín, from the animal facility at CITIUS (Universidad de Sevilla). The authors wish to give a special thanks to the late Dr. Oscar Pintado for pronuclear injection.

References

Andrade-Talavera, Y., et al., 2015. Rapamycin restores BDNF-LTP and the persistence of long-term memory in a model of Down's syndrome. Neurobiol. Dis. 82, 516–525.
Andreescu, C.E., et al., 2007. Estradiol improves cerebellar memory formation by activating estrogen receptor beta. J. Neurosci. 27, 10832–10839.
Arruda-Carvalho, M., Clem, R.L., 2014. Pathway-selective adjustment of prefrontal-amygdala transmission during fear encoding. J. Neurosci. 34, 15601–15609.
Barthet, G., Mulle, C., 2020. Presynaptic failure in Alzheimer's disease. Prog. Neurobiol. 194, 101801.
Barthet, G., et al., 2018. Presenilin-mediated cleavage of APP regulates synaptotagmin-7 and presynaptic plasticity. Nat. Commun. 9, 4780.
Bot, N., et al., 2011. Processing of the synaptic cell-adhesion molecule neurexin-3{beta} by Alzheimer's disease {alpha}- and {gamma}-secretases. J. Biol. Chem. 286, 2762–2773.
Bozeat, S., et al., 2000. Which neuropsychiatric and behavioural features distinguish frontal and temporal variants of frontotemporal dementia from Alzheimer's disease? J. Neurol. Neurosurg. Psychiatry 69, 178–186.
Burgos-Robles, A., et al., 2009. Sustained conditioned responses in prelimbic prefrontal neurons are correlated with fear expression and extinction failure. J. Neurosci. 29, 8474–8482.
Cacace, R., et al., 2016. Molecular genetics of early-onset Alzheimer's disease revisited. Alzheimers Dement. 12, 733–748.
Camacho-Garcia, R.J., et al., 2012. Mutations affecting synaptic levels of neurexin-1beta in autism and mental retardation. Neurobiol. Dis. 47, 135–143.
Camacho-Garcia, R.J., et al., 2013. Rare variants analysis of neurexin-1beta in autism reveals a novel start codon mutation affecting protein levels at synapses. Psychiatr. Genet. 23, 262–266.
Cao, T., et al., 2018. Histone deacetylase inhibitor alleviates the neurodegenerative phenotypes and histone dysregulation in presenilins-deficient mice. Front. Aging Neurosci. 10, 137.
Carlin, R.K., et al., 1980. Isolation and characterization of postsynaptic densities from various brain regions: enrichment of different types of postsynaptic densities. J. Cell Biol. 86, 831–845.
Cerejeira, J., et al., 2012. Behavioral and psychological symptoms of dementia. Front. Neurol. 3, 73.
Corcoran, K.A., Quirk, G.J., 2007. Activity in prelimbic cortex is necessary for the expression of learned, but not innate, fears. J. Neurosci. 27, 840–844.
De Strooper, B., 2007. Loss-of-function presenilin mutations in Alzheimer disease. Talking Point on the role of presenilin mutations in Alzheimer disease. EMBO Rep. 8, 141–146.
Dean, C., et al., 2003. Neurexin mediates the assembly of presynaptic terminals. Nat. Neurosci. 6, 708–716.
Duits, F.H., et al., 2018. Synaptic proteins in CSF as potential novel biomarkers for prognosis in prodromal Alzheimer's disease. Alzheimers Res. Ther. 10, 5.
Erdmann, G., et al., 2007. Inducible gene inactivation in neurons of the adult mouse forebrain. BMC Neurosci. 8, 63.
Feng, R., et al., 2004. Forebrain degeneration and ventricle enlargement caused by double knockout of Alzheimer's presenilin-1 and presenilin-2. Proc. Natl. Acad. Sci. U. S. A. 101, 8162–8167.
Franklin, K.B.J., Paxinos, G., 2007. The Mouse Brain in Stereotaxic Coordinates, 3rd ed. Elsevier Academic Press.
Goetzl, E.J., et al., 2018. Declining levels of functionally specialized synaptic proteins in plasma neuronal exosomes with progression of Alzheimer's disease. FASEB J. 32, 888–893.
Gomez, A.M., et al., 2021. Neurexins: molecular codes for shaping neuronal synapses. Nat. Rev. Neurosci. 22, 137–151.
Gruart, A., et al., 2006. Involvement of the CA3-CA1 synapse in the acquisition of associative learning in behaving mice. J. Neurosci. 26, 1077–1087.
Guilmatre, A., et al., 2009. Recurrent rearrangements in synaptic and neurodevelopmental genes and shared biologic pathways in schizophrenia, autism, and mental retardation. Arch. Gen. Psychiatry 66, 947–956.
Güner, G., Lichtenthaler, S.F., 2020. The substrate repertoire of γ-secretase/presenilin. Semin. Cell Dev. Biol. 105, 27–42.
Gureviciene, I., et al., 2004. Normal induction but accelerated decay of LTP in APP + PS1 transgenic mice. Neurobiol. Dis. 15, 188–195.
Haapasalo, A., Kovacs, D.M., 2011. The many substrates of presenilin/γ-secretase. J. Alzheimers Dis. 25, 3–28.
Han, H.J., et al., 2012. Strain background influences neurotoxicity and behavioral abnormalities in mice expressing the tetracycline transactivator. J. Neurosci. 32, 10574–10586.
Harrison, F.E., et al., 2009. Endogenous anxiety and stress responses in water maze and Barnes maze spatial memory tasks. Behav. Brain Res. 198, 247–251.
Huang, Y.Y., Kandel, E.R., 1998. Postsynaptic induction and PKA-dependent expression of LTP in the lateral amygdala. Neuron. 21, 169–178.
Hübner, C., et al., 2014. Ex vivo dissection of optogenetically activated mPFC and hippocampal inputs to neurons in the basolateral amygdala: implications for fear and emotional memory. Front. Behav. Neurosci. 8, 64.
Humeau, Y., et al., 2003. Presynaptic induction of heterosynaptic associative plasticity in the mammalian brain. Nature. 426, 841–845.
Katz, B., Miledi, R., 1968. The role of calcium in neuromuscular facilitation. J. Physiol. 195, 481–492.
Kim, J.J., Fanselow, M.S., 1992. Modality-specific retrograde amnesia of fear. Science. 256, 675–677.
Lauri, S.E., et al., 2007. Presynaptic mechanisms involved in the expression of STP and LTP at CA1 synapses in the hippocampus. Neuropharmacology. 52, 1–11.
Lee, S.H., et al., 2017. Presenilins regulate synaptic plasticity and mitochondrial calcium homeostasis in the hippocampal mossy fiber pathway. Mol. Neurodegener. 12, 48.
Lleó, A., et al., 2019. Changes in synaptic proteins precede neurodegeneration markers in preclinical Alzheimer's disease cerebrospinal fluid. Mol. Cell. Proteomics 18, 546–560.
Madroñal, N., et al., 2009. Differing presynaptic contributions to LTP and associative learning in behaving mice. Front. Behav. Neurosci. 3, 7.
Martinez-Mir, A., et al., 2013. Genetic study of neurexin and neuroligin genes in Alzheimer's disease. J. Alzheimers Dis. 35, 403–412.
Mayford, M., et al., 1996. Control of memory formation through regulated expression of a CaMKII transgene. Science. 274, 1678–1683.
Nicholls, R.E., et al., 2008. Transgenic mice lacking NMDAR-dependent LTD exhibit deficits in behavioral flexibility. Neuron. 58, 104–117.
Peixoto, R.T., et al., 2012. Transsynaptic signaling by activity-dependent cleavage of neuroligin-1. Neuron. 76, 396–409.
Phillips, R.G., LeDoux, J.E., 1992. Differential contribution of amygdala and hippocampus to cued and contextual fear conditioning. Behav. Neurosci. 106, 274–285.
Prioni, S., et al., 2012. Stereotypic behaviors in degenerative dementias. J. Neurol. 259, 2452–2459.
Rabaneda, L.G., et al., 2014. Neurexin dysfunction in adult neurons results in autistic-like behavior in mice. Cell Rep. 8, 338–346.

Roberts, A.C., et al., 2009. Downregulation of NR3A-containing NMDARs is required for synapse maturation and memory consolidation. Neuron. 63, 342–356.
Rodgers, S.P., et al., 2012. Transgenic APP expression during postnatal development causes persistent locomotor hyperactivity in the adult. Mol. Neurodegener. 7, 28.
Rujescu, D., et al., 2009. Disruption of the neurexin 1 gene is associated with schizophrenia. Hum. Mol. Genet. 18, 988–996.
Saura, C.A., et al., 2004. Loss of presenilin function causes impairments of memory and synaptic plasticity followed by age-dependent neurodegeneration. Neuron. 42, 23–36.
Saura, C.A., et al., 2011. Presenilin/gamma-secretase regulates neurexin processing at synapses. PLoS One 6, e19430.
Schreiner, D., et al., 2014. Targeted combinatorial alternative splicing generates brain region-specific repertoires of neurexins. Neuron. 84, 386–398.
Servián-Morilla, E., et al., 2018. Proteolytic processing of Neurexins by presenilins sustains synaptic vesicle release. J. Neurosci. 38, 901–917.
Shen, J., Kelleher 3rd, R.J., 2007. The presenilin hypothesis of Alzheimer's disease: evidence for a loss-of-function pathogenic mechanism. Proc. Natl. Acad. Sci. U. S. A. 104, 403–409.
Shen, J., et al., 1997. Skeletal and CNS defects in Presenilin-1-deficient mice. Cell. 89, 629–639.
Silverman, J.L., et al., 2010. Behavioural phenotyping assays for mouse models of autism. Nat. Rev. Neurosci. 11, 490–502.
Sotres-Bayon, F., Quirk, G.J., 2010. Prefrontal control of fear: more than just extinction. Curr. Opin. Neurobiol. 20, 231–235.
Südhof, T.C., 2017. Synaptic Neurexin complexes: a molecular code for the logic of neural circuits. Cell. 171, 745–769.
Sun, L., et al., 2017. Analysis of 138 pathogenic mutations in presenilin-1 on the in vitro production of Aβ42 and Aβ40 peptides by γ-secretase. Proc. Natl. Acad. Sci. U. S. A. 114, E476–e485.
Suzuki, K., et al., 2012. Activity-dependent proteolytic cleavage of neuroligin-1. Neuron. 76, 410–422.
Szatmari, P., et al., 2007. Mapping autism risk loci using genetic linkage and chromosomal rearrangements. Nat. Genet. 39, 319–328.
Thomson, A.M., 2000. Facilitation, augmentation and potentiation at central synapses. Trends Neurosci. 23, 305–312.
Treutlein, B., et al., 2014. Cartography of neurexin alternative splicing mapped by single-molecule long-read mRNA sequencing. Proc. Natl. Acad. Sci. U. S. A. 111. E1291-e1299.
Wolfe, M.S., 2007. When loss is gain: reduced presenilin proteolytic function leads to increased Abeta42/Abeta40. Talking Point on the role of presenilin mutations in Alzheimer disease. EMBO Rep. 8, 136–140.
Xia, D., et al., 2015. Presenilin-1 knockin mice reveal loss-of-function mechanism for familial Alzheimer's disease. Neuron. 85, 967–981.
Zhang, C., et al., 2009. Presenilins are essential for regulating neurotransmitter release. Nature. 460, 632–636.
Zhou, R., et al., 2017. Dominant negative effect of the loss-of-function γ-secretase mutants on the wild-type enzyme through heterooligomerization. Proc. Natl. Acad. Sci. U. S. A. 114, 12731–12736.
Zucker, R.S., Regehr, W.G., 2002. Short-term synaptic plasticity. Annu. Rev. Physiol. 64, 355–405.